CHAPTER III
SELF-FORMATION OF 3D INTERCONNECTED MACROPOROUS CARBON XEROGELS DERIVED FROM POLYBENZOXAZINE BY SELECTIVE SOLVENT DURING THE SOL-GEL PROCESS

3.1 Abstract

Polybenzoxazine (PBZ)-based carbon xerogel has been synthesized by a sol-gel process and carbonization. By using different solvents, the microstructure of the porous carbon can be tailored for a wide range of desired properties. In addition, a new aspect to produce 3D-interconnected macroporous carbon xerogels by using selective solvent via self-formation is introduced. Dimethylformamide (DMF), dioxane, and isopropanol are separately used as a solvent during a sol-gel process. The SEM micrographs reveal different structures of carbon xerogel depending on the type of solvent used. By using DMF as a solvent during a sol-gel process and ambient pressure drying, the carbon xerogel shows a similar porous structure to that of a PBZ-based carbon aerogel obtained through supercritical CO_2 drying. In the DMF system, a short gelation time is observed (1.15-3 h) due to the fast ring-opening polymerization accelerated by DMF resulting in the formation of 3D-interconnected macroporous structure without using any template. Comparing the rates of cluster growth between DMF and dioxane systems, the rate of cluster growth in dioxane system is slower than that of DMF system, implying good miscibility between PBZ and dioxane. Moreover, microporous spherical particles are obtained from the isopropanol system due to the self-micelle-like formation.

3.2 Introduction

Macroporous carbon with 3D interconnected structure is an interesting macroporous material because of its outstanding properties compared to those like silica monolith or polymer monolith. Some of these attractive properties are: high resistance to acidic and basic conditions, sufficient mechanical integrity, lack of swelling effects, thermal stability, low pressure drop during operation, 3D-opened porous structure, and good mass transfer. Due to macroporous carbon's exceptional properties, there are great opportunities for it to be used in various advanced applications. These applications include thermal insulation, water purification, continuous flow operation catalyst support, liquid fuel cells electrocatalyst support [1], and especially HPLC columns [2]. Normally, macroporous carbons are produced by using various methods and templates, such as ultrasonic irradiation [3-5], micronsized silica beads [2], colloidal silica [6], polystyrene microspheres [1, 7], and silica monolith/mesoporous silica [8, 9]. However, the removal process of those templates from macroporous carbon requires a multi-step procedure, includes the risk of using acids and bases during the process, and leads to considerable production cost by consuming time and energy. The multi-step process and extensive production cost might be one of the important factors that limit the further utilization of macroporous carbon on an industrial scale.

Many researchers have reported the synthesis of macroporous carbon based on polycondensation of resorcinol (R) and formaldehyde (F) [2-5, 7]. Generally, a volatile by-product was released during the polymerization process of a RF polymer [10-12]. In addition, a base catalyst and supercritical/freeze drying were required to promote polymerization and remove solvent to preserve the porous structure. Even if the pore structure of gels could be maintained, supercritical/freeze drying is still not a cost-effective drying method. Not only does it require a multi-step procedure, but it also yields a low production rate, resulting in a substantial amount of time and energy consumption. Recently, there have been many attempts to simplify the drying process by using supercritical acetone and alcoholic sol-gel processes [13-15]. Nevertheless, in comparison to supercritical drying, ambient pressure drying method is much more cost-effective, although the morphology and physical properties of the

ambient-dried products are typically different from those obtained by supercritical drying [16-20].

Polybenzoxaxine (PBZ), a new type of cationic ring-opening polymerized phenolic system, has many excellent properties that overcome several shortcomings of traditional phenolic resin. Benzoxazine resins do not require harsh catalysts, do not release toxic by-products during polymerization, show near-zero shrinkage upon polymerization, and possess easy processibility. Cross-linked polybenzoxazines exhibit excellent mechanical integrity, high thermal and chemical stability, high char yield, and low water absorption [21-25]. These properties enable polybenzoxazines to be good candidates as precursors for preparing carbon xerogels. In addition, polybenzoxazine has superb molecular design flexibility. By changing either types of phenol or amine used as starting materials, the pore structure of organic and carbon aerogels can be tailored for a wide range of desired properties.

In 2009, Lorjai et al. first reported the synthesis of polybenzoxazine-based aerogel derived from bisphenol-A and aniline by a sol-gel process using xylene as a solvent. They found that the unactivated carbon aerogel obtained after pyrolysis was a microporous material with the BET surface area of around 384-391 m^2/g [26].

In 2010, polybenzoxazine-based carbon aerogels were used as electrodes for supercapacitors by Katanyoota et al. [27]. They compared polybenzoxazine-based carbon aerogel derived from bisphenol-A – aniline (hereinafter abbreviated as BA-a) and bisphenol-A – teta (hereinafter abbreviated as BA-teta), and found that carbon aerogel derived from BA-teta showed higher mesoporosity than those derive from BA-a.

Polybenzoxazine-based carbon aerogel was further reported in 2012 by Rubenstein et al. [28]. They studied the physical properties of pure polybenzoxazine and benzoxazine that was copolymerized with resorcinol and formaldehyde, their conversion characteristics to carbon aerogels, and the biocompatibility of the subsequent carbon aerogels with human osteoblasts.

It is known that many parameters can affect the properties of organic xerogels during the phase separation process and its carbon xerogels after carbonization as well. According to our previous work [29], one of the most important parameters affecting the pore structure of carbon xerogels is the difference

in the solubility parameters between the solvent and polymer since the formation behavior of polymer cluster during the phase separation process varies with different solvents, yielding different morphologies and properties [29-33]. A polymer in a good solvent system prefers being miscible, resulting in the generation of smaller pore and dense structure while a polymer in a poor solvent system (θ-solvent) prefers aggregating to each other and separating out from the solvent as soon as possible, resulting in the 3D interconnected macropore structure.

In this work, we aim to produce 3D interconnected macroporous carbon xerogels from polybenzoxazine and ambient pressure drying method. Moreover, the new aspect – selective solvent method for producing 3D interconnected macroporous carbon xerogels – is introduced. By using selective solvents and applying the knowledge of phase separation behavior between polybenzoxazine and solvents during the sol-gel process, the 3D interconnected macropore structure of organic/carbon xerogels can be readily produced during the sol-gel process by self-formation of superstructures having various pore structures without the need of any hard template or external ultrasonic irradiation.

Normally, solvents are classified into three types, nonpolar, polar aprotic, and polar protic. In this investigation, three solvents were used, dimethylformamide (DMF, representative of polar aprotic solvent), dioxane (representative of nonpolar solvent), and isopropanol (representative of polar protic solvent). The effects of these solvents on the cluster growth behaviors during the sol-gel process, the pore characteristics of polybenzoxazine-derived xerogels, and their corresponding carbon xerogels, were studied in order to obtain knowledge about the controlling parameters of the pore structure of PBZ-based carbon xerogels for targeted applications. The effects of resin concentrations and drying methods were also investigated.

3.3 Experimental

3.3.1 Materials

Polybenzoxazines used in this work were synthesized by the Mannich condensation reaction between bisphenol-A [BA, $(CH_3)_2C(C_6H_4OH)_2$], triethylenetetramene [teta, $(CH_2NHCH_2CH_2NH_2)_2$], and formaldehyde (CH_2O) using dioxane ($C_4H_8O_2$), isopropanol [$(CH_3)_2CHOH$], and dimethylformamide [DMF, $(CH_3)_2NC(O)H$] as solvents. Bisphenol-A (97%) was purchased from Aldrich. Formaldehyde (37% w/w) was purchased from Merck Limited, Germany, and teta (85%) was purchased from Facai Group Limited, Thailand. Dioxane (>99.8%), isopropanol (>99.9%), and DMF (>99.8%) were purchased from Labscan Asia Co., Ltd., Thailand (analytical grade). All chemicals were used without further purification.

3.3.2 Synthesis of polybenzoxazine-based carbon xerogels (PBZ-based carbon xerogels)

3.3.2.1 Synthesis of main-chain type benzoxazine polymer (MCBP) organogels

A main-chain type benzoxazine polymer (MCBP) with benzoxazine groups as part of the chemical repeating units was used as a precursor for carbon xerogel preparation. The MCBP was synthesized by a quasi-solventless method adapted from the solventless method proposed by Ishida [34]. The synthesis of MCBP was based on a molar ratio of 1:1:4 of the reaction between bisphenol-A, teta, and formaldehyde, respectively. Unlike the conventional method which took 5 h, the reaction was completed within an hour [35]. The main-chain type linear polybenzoxazine derived from bisphenol-A and teta is hereinafter abbreviated as MCBP(BA-teta). The polycondensation reaction of MCBP(BA-teta) was shown in our previous publications [29, 36]. To study the effect of solvent types, bisphenol-A was separately dissolved in different solvents, and magnetically stirred for 20 min; then formaldehyde was mixed into the bisphenol-A mixture and stirred for additional

20 min. Subsequently, teta was added dropwise into the mixture which was then continuously stirred in an ice bath where the temperature was kept at 10 °C. After 1 h, the transparent pale yellow MCBP(BA-teta) solution was obtained which was transferred into a glass vial and sealed. The solution was left in a closed system for 1 day prior to heating in an oil bath at 80 °C for 2 days to let the gel set, resulting in a white opaque MCBP(BA-teta) organogel [29]. It should be noted that the MCBP(BA-teta) concentration was kept constant at 25 % w/w in order to study the effects of solvents. On the other hand, to investigate the effect of resin concentration, the resin concentration was varied at 25%, 35%, and 45% w/w while DMF was used commonly as the solvent.

3.3.2.2 Drying, polymerization, and pyrolysis process

Synthesized organogels were taken out of glass vials and cut into disk shape prior to drying under ambient pressure with air flow for 72 h. Then, the organogels were placed in an oven for step-polymerization at 160 °C and 180 °C for 3 h at each temperature, and 200 °C for 1 h to achieve the fully–polymerized polybenzoxazine xerogel [27]. The fully-polymerized xerogels were pyrolyzed under a nitrogen flow of 600 cm^3/min using the following ramp cycle: 30–250 °C for 1 h, 250–600 °C for 5 h, 600–800 °C for 1 h, and hold at 800 °C for 2 h. Subsequently, the oven was cooled to room temperature under nitrogen atmosphere. Polybenzoxazine-based carbon xerogels using dioxane, isopropanol, and DMF as solvents during the synthesis of MCBP(BA-teta) solution are denoted as C-DiX-xx, C-IX-xx, and C-DX-xx, where DiX, IX, and DX are the abbreviation for dioxane, isopropanol, and DMF, by ambient pressure drying (X=Xerogel), respectively. The last abbreviation (-xx) shows the benzoxazine concentration by weight percentage.

For the DMF system, the MCBP(BA-teta) concentration was kept constant at 35 % w/w and supercritical CO_2 drying was also used to investigate the effect of different drying processes. The resulting carbon from the DMF system was denoted as C-DA-35 indicating that DMF was used as a solvent during the synthesis of MCBP(BA-teta) solution and the organogel was dried under supercritical CO_2 drying before polymerization and carbonization.

3.3.3 Characterizations of polybenzoxazine-based carbon xerogels

3.3.3.1 Measurements of gelation time, cluster size, and density

The cluster size of MCBP(BA-teta) during phase separation phenomena was measured by dynamic light scattering technique (DLS) using a Malvern Zetasizer Nano Series (Malvern Instruments Ltd.) with a detection angle of 173°. In general, the gelation point is the infinite connection of molecules or superstructures resulting in a white opaque organogel, which does not let the light pass through. Consequently, the DLS technique was not used to measure the size of the infinite connection of clusters at the gelation point. In this study, the gelation point/time was determined visually when the solution became white-opaque and lost its flow at ambient condition. The cluster growth behavior of the MCBP(BA-teta) solution was observed by recordings of the cluster sizes starting after the MCBP(BA-teta) solution was stirred for 1 h and sealed in a closed system until the MCBP(BA-teta) solution turned to white-opaque (viscous liquid and almost reaching gelation point) in which DLS technique could not be used. At this point, the recorded time is called "pseudo-gelation time" (pseudo-gelation point), which is slightly shorter – about 10 minutes shorter for DMF system and 3 hours shorter for dioxane system – than gelation time. Therefore, the final cluster size observed by the DLS technique is the size measured at the pseudo-gelation time.

The skeletal density (ρ_s) of samples was measured by gas pycnometer (Ultrapycnometer, Quantachrome Instrument). The mass (m) and volume (V) of samples were measured and the bulk density (ρ) was calculated from the following formula.

$$\rho = m / V \tag{1}$$

3.3.3.2 Identification of microstructure and morphology of polybenzoxazine-based carbon xerogels

The morphology and microstructure of carbon xerogels were identified by field emission scanning electron microscope (FE-SEM, Hitachi/S-4800 model). The samples were coated with platinum before examination. The

microstructure of carbon gels was also observed by transmission electron microscope (TEM, JEOL 2010F). Quantachrome-Autosorp1-MP was used to determine the adsorption-desorption properties and porous structure of the samples. Approximately 0.1 g of carbon xerogel was degassed at 250 °C for 15 h to remove all adsorbed gas species. The specific surface area (S_{BET}) was calculated by BET (Brunauer-Emmett-Teller) algorithm [37]. The micropore volume (V_{mic}) and micropore surface area (S_{mic}) were analyzed by the t-plot method at a relative pressure (see equation 4 in a later section for the definition) of less than 0.1 [38]. The micropore size distribution was analyzed by the MP method (Standard micropore size distribution). Mesopore volume (V_{mes}) and mesopore size distribution were analyzed by the BJH (Barrett-Joyner-Halenda) algorithm [39, 40]. In addition, mesopore volume was also calculated from the subtraction of the adsorbate amount at a relative pressure of 0.1 from that at a relative pressure of 0.95 [41, 42]. Macropore volume (V_{mac}) and total pore volume were calculated according to the method of Wu et al. [43], in which the total pore volume was determined from the following equation: $V_{total} = (1/\rho) - (1/\rho_s)$ where ρ is the bulk density and ρ_s is the skeletal density. Macropore volume was determined by the subtraction of total pore volume from micro- and meso- pore volume as shown in the following equation [43]: $V_{mac} = V_{total} - V_{meso} - V_{micro}$.

3.4 Results and Discussion

3.4.1 Effects of solvents

3.4.1.1 Gelation, densities, and morphologies

The most important parameter affecting the pore structure during phase separation is the difference in solubility parameters between solvent and polymer. The time corresponding to the sol-gel transition, which is related to the rate of cluster growth, can be expressed by the gelation time. During the gelation process, the molecular weight of benzoxazine resin increases, resulting in the formation and growth of benzoxazine clusters. Finally, gelation is achieved by

connecting the benzoxazine clusters which are surrounded by the solvent [10, 44, 45]. The solvent that is present in the interstices of the clusters is subsequently dried by an economical, ambient pressure drying method, resulting in the creation of pores. In other words, the gelation process takes place by phase separation of cross-linked polybenzoxazines and aggregation of phase-separated particles as the morphology of the polymeric gel depends on the difference in solubility parameter between the solvent and polymer.

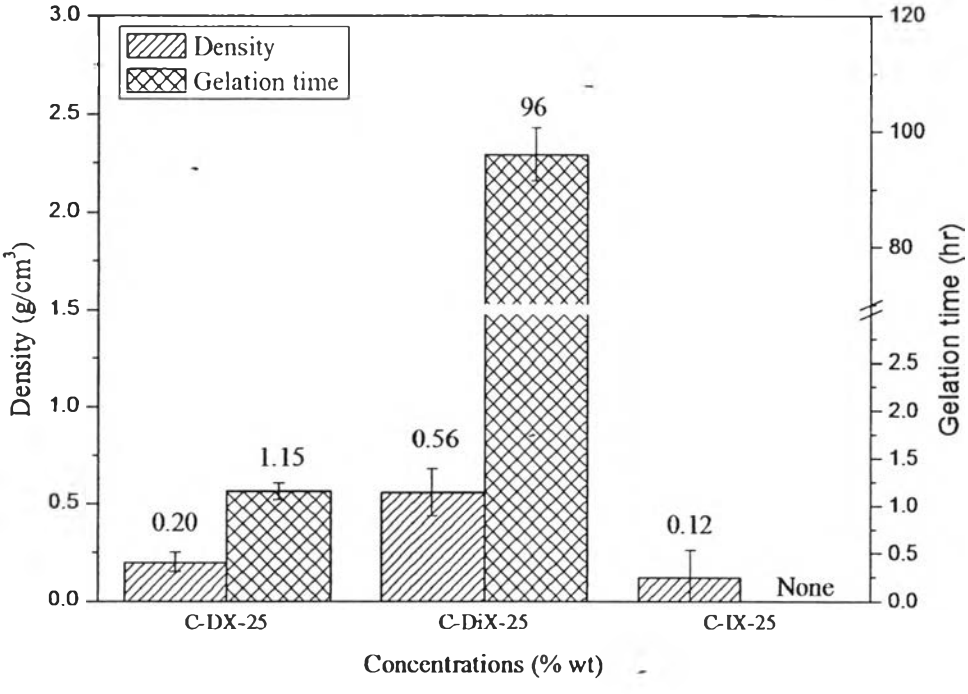

Figure 3.1 Densities and gelation times of carbon xerogels at 25 % w/w using DMF (C-DX-25), dioxane (C-DiX-25), and isopropanol (C-IX-25) as solvents by ambient pressure drying.

In this work, the three solvents used were DMF, dioxane, and isopropanol. The concentration of benzoxazine was kept at 25% w/w. The density and gelation time are shown in Figure 3.1. Carbon xerogel derived from the dioxane system (abbreviated as C-DiX-25) shows the highest density around 0.56 g/cm^3 followed by 0.20 g/cm^3 and 0.12 g/cm^3 for carbon xerogel derived from DMF (abbreviated as C-DX-25) and isopropanol (abbreviated as C-DIX-25) systems,

respectively. C-DiX-25 exhibits a gelation time of 96 h (4 days) and, in a DMF system, C-DX-25 surprisingly shows a shorter gelation time of 1.15 h. Moreover, the gelation time is shortened to less than 10 minutes for a DMF system and 4 h for a dioxane system, when the MCBP(BA-teta) solution was heated at 80 °C. However, for C-IX-25, after 25 h in a closed system, precipitation took place. Therefore, the cluster size reported in this work was determined for 24 h prior to the precipitation, and the gelation time of C-IX-25 (at ambient condition) was not reported. From Figure 3.2, at the pseudo-gelation point, the cluster sizes of 2880 nm, 1150 nm, and 140 nm were observed for C-IX-25, C-DX-25, and C-DiX-25, respectively.

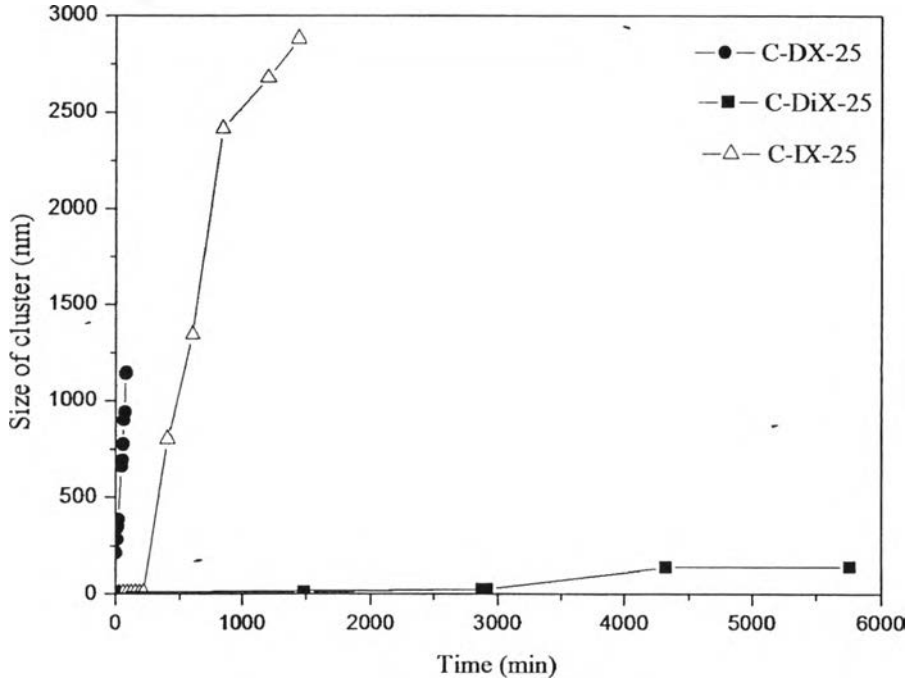

Figure 3.2 Size of cluster during gelation process at 25 %w/w using DMF (C-DX-25), dioxane (C-DiX-25), and isopropanol (C-IX-25) as solvents.

The difference in the gelation times might be caused by different solubility parameters between MCBP(BA-teta) and the solvents. The solubility parameter concept is based on the heat of vaporization proposed by Hildebrand et al. as follows [46, 47]:

$$\frac{\Delta E_{mix}}{\phi_1 \phi_2} = V_m (\delta_1 - \delta_2)^2 \quad (2)$$

$$\delta = \left[\frac{\Delta E_{vap}}{V_m} \right]^{1/2} \quad (3)$$

where δ_1 and δ_2 = solubility parameter (such as polymer and solvent), V_m = average molar volume based on mole fraction, ϕ_1 and ϕ_2 = volume fraction of material 1 and 2, respectively, ΔE_{mix} = Energy of mixing, and ΔE_{vap} = heat of vaporization. Equation 2 provides the prediction of the energy of mixing between polymer and solvent, based on the solubility parameters (δ_1 and δ_2) – which were calculated from equation 3 – of two single components [46, 47].

Therefore, the difference in solubility parameters, $\delta_1 - \delta_2$, can be used to predict the miscibility between polymer and solvent. The universal solubility parameters of DMF, dioxane, and isopropanol are 12.1, 10.0, and 8.8 $(cal/cm^3)^{1/2}$, respectively. For C-DiX-25, the longer gelation time (Figure 3.1) and the smallest cluster size during the gelation time (Figure 3.2) imply that the solubility parameter of benzoxazine precursor (δ_1) is close to the solubility parameter of dioxane (δ_2), yielding small $\Delta\delta$ which leads to good miscibility. As a result, it was rather difficult for the phase separation to take place. Therefore, the longer gelation time and smallest cluster size were obtained when dioxane was used as a solvent. Moreover, C-DiX-25 shows highly dense morphology and small amounts of pores were created (Figure 3.3c) due to the structural collapse during ambient drying. The good interaction between MCBP(BA-teta) and dioxane as described earlier might be the cause of this phenomenon (see Figure 3.2).

When DMF was used as a solvent, an interestingly shorter gelation time of 1.15 h and large cluster size of about 1150 nm were observed, implying a large difference in solubility parameters ($\Delta\delta$) between benzoxazine precursor and DMF, leading to poor miscibility. Therefore, benzoxazine primary particles are easy to separate out from DMF and aggregate to each other, resulting in the 3D interconnected macroporous structure (Figure 3.3a).

In other words, the difference in gelation time of polybenzoxazine in DMF and dioxane system is, in part, related to the tendency of oxazine ring-opening. Oxazine rings tend to open in solvents with large dielectric constants such as hydrophilic solvents like DMF, whereas in a solvent, such as dioxane with low dielectric constant, it is more difficult to open. Thus, the formation of extended molecular structure is easier to achieve in DMF than in dioxane [29]. 3D interconnected marcroporous carbon xerogels were easily obtained from the DMF system after the removal of solvent as shown in Figure 3.3a. Whereas, in the dioxane system, shown in Figure 3.3b, the structure of carbon xerogels was totally dominated by mesoporous structure.

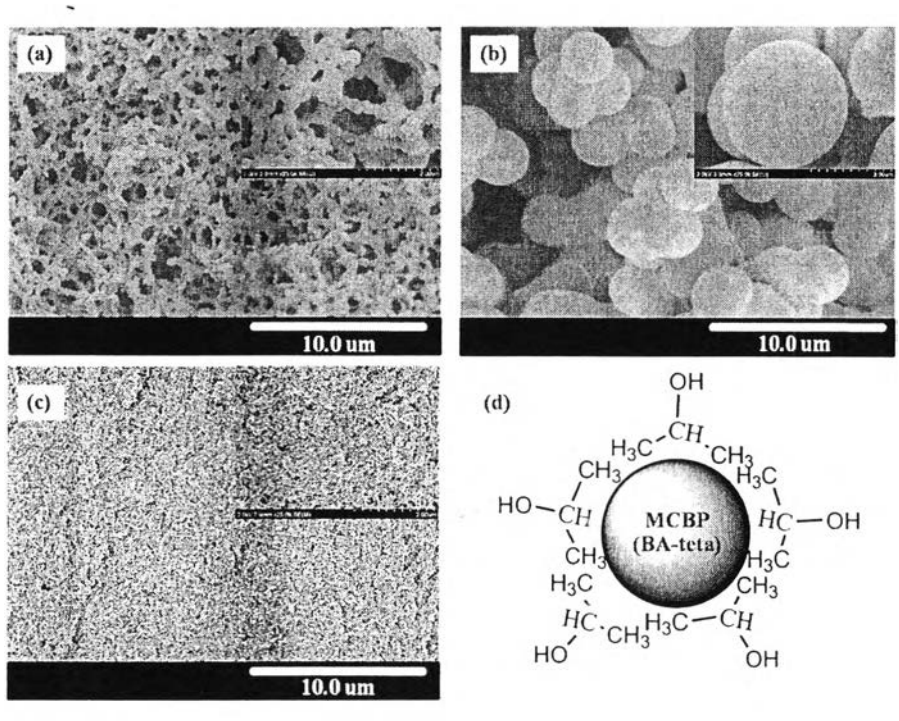

Figure 3.3 SEM micrographs of carbon xerogels using DMF, isopropanol, and dioxane as solvents by ambient pressure drying (inset: high magnification) (a) C-DX-25 (b) C-IX-25 (c) C-DiX-25 (d) self-micelle-like formation model.

In the case of C-IX-25 where isopropanol was used as a solvent, microspherical particles were also obtained (Figure 3.3b); this is interesting because they were produced without the need of surfactants and inverse phase

process to form micelle, as usually seen in other literature [48-51]. The average size of the microspherical particles, obtained from SEM, was about 2.5 μm. The microspherical particles were loosely packed together, and a large opened structure was created. Therefore, mesopores and micropores of C-IX-25 should be generated on the microspherical particles rather than being generated by interconnected particles as described in other studies [44, 52-54]. However, some microspherical particles tend to agglomerate. The proposed model for the spherical formation of C-IX-25 was the self-micelle-like formation by the solvent (isopropanol) as shown in Figure 3.3d. According to the like-dissolves-like model, the methyl group of isopropanol acted as inner cores of micelle having benzoxazine precursor inside and the outer core was hydroxyl group of isopropanol.

3.4.1.2 Microstructure of polybenzoxazine-based carbon xerogels

Figure 3.4a shows the N_2 adsorption-desorption isotherms of xerogels prepared from different solvents at a constant benzoxazine concentration. According to the IUPAC classification, C-DX-25 exhibits the combination isotherm of type IIb with a H3 hysteresis loop and type Ic in which type Ic represents microporous adsorbent containing mesopores and type IIb represents macroporous adsorbent [52, 53, 55]. C-IX-25 exhibits the adsorption isotherms of type Ib with a H4 hysteresis loop and low relative pressure hysteresis loop [52, 53, 55]. The type Ib corresponds to microporous material. The H4 hysteresis loop represents the slit-shaped pore [53, 55]. As shown in Table 3.1, C-IX-25 has the micropore size of 1.36 nm with micropore volume of 0.16 cm^3/g, indicating that it is supermicroporous (0.7-2 nm); as such, capillary condensation could have taken place. However, the BET surface area obtained from C-IX-25 should be carefully interpreted because the BET theory is not appropriate for microporous materials.

From the original IUPAC classification, the adsorption isotherm of C-DiX-25 exhibits the characteristic of type IVa which represents mesoporous material with an obvious H1 hysteresis loop (Figure 3.4a), indicating a narrow distribution of uniform pores. In addition, the adsorption characteristic of C-DiX-25 reaches the plateau regime, implying that this carbon contains no macropores.

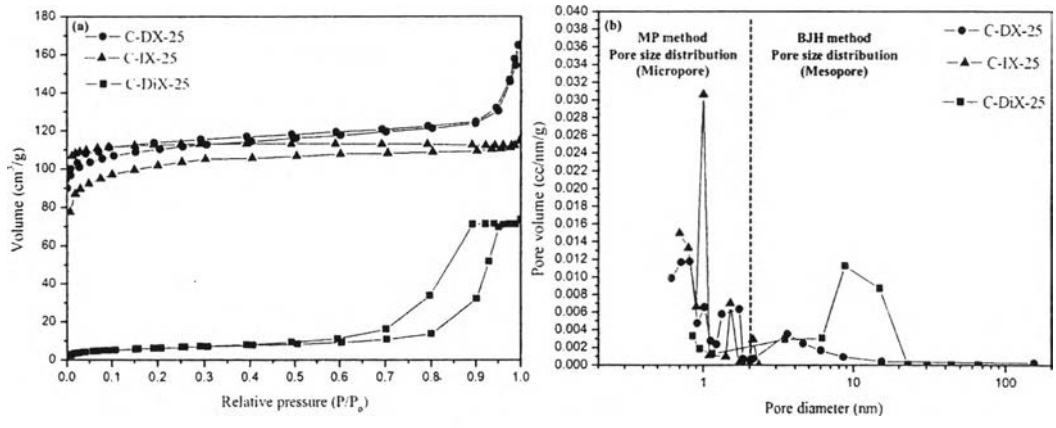

Figure 3.4 (a) N_2 adsorption-desorption isotherms of carbon xerogels using DMF (C-DX-25), dioxane (C-DiX-25), and isopropanol (C-IX-25) as solvents by ambient pressure drying (b) pore size distribution.

Table 3.1 Pore characteristics of carbon xerogels using different solvents by ambient pressure drying at 25% w/w of solid contents

Sample	S_{BET} (m^2/g)	S_{micro} (m^2/g)	V_{micro} (cm^3/g)	V_{meso} (cm^3/g)	V_{macro} (cm^3/g)	V_{total} (cm^3/g)	APD_{micro} (nm)	APD_{meso} (nm)
C-DX-25	337	291	0.15	0.08	4.33	4.56	1.16	3.65
C-DiX-25	22	86	0.03	0.13	0.05	0.21	0.97	8.79
C-IX-25	318	306	0.16	-	7.61	7.77	1.36	-

Note : S_{BET} : BET surface area ; S_{micro} : micropore surface area ; V_{micro} : micropore volume ; V_{meso} : mesopore volume ; V_{macro} : macropore volume ; V_{total} : total pore volume ; APD_{micro} : average micropore diameter ; APD_{meso} : average mesopore diameter

The pore characteristics of C-DiX-25 are summarized in Table 3.1. The total pore volume and specific surface area of C-DiX-25 (0.21 cm^3/g, 22 m^2/g) are too low to compare to those of C-DX-25 (4.56 cm^3/g, 337 m^2/g) and C-IX-25 (7.77 cm^3/g, 318 m^2/g); this low volume and specific surface area might be due to the strong interaction (small $\Delta\delta$) between benzoxazine and dioxane, resulting in pore collapse during solvent removal process. The SEM micrograph in Figure 3.3c supports the results obtained from the N_2 adsorption measurements (Figure 3.4 and Table 3.1). In addition, an extremely large macropore volume of 4.33 cm^3/g can be

obtained from 3D interconnected macroporous carbon xerogel synthesized in DMF system (C-DX-25).

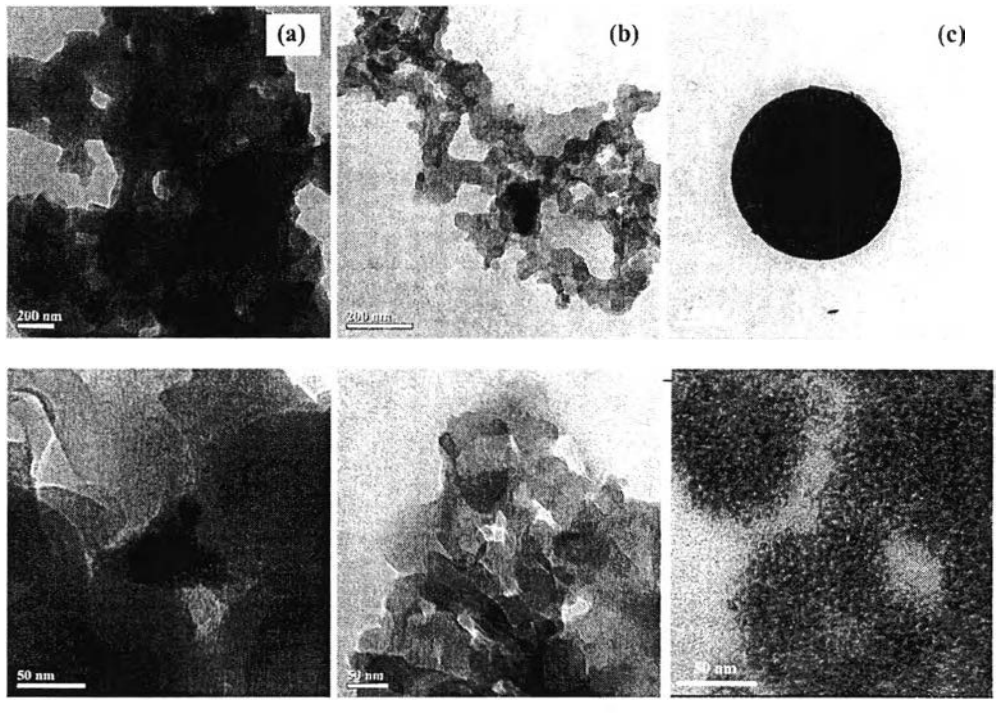

Figure 3.5 TEM images of carbon xerogels at 25% w/w (a) C-DX-25 (b) C-DiX-25 (c) C-IX-25; upper: low magnification; lower: high magnification.

TEM images are shown in Figure 3.5. Figures 3.5a and 5b represent the interconnected structure of cross-linked MCBP(BA-teta) clusters generated during the phase separation process. Moreover, Figure 3.5a (at high magnification) shows the small primary clusters aggregated as secondary clusters which generate a small average pore diameter of 3.65 nm and is consistent with the SEM micrograph in Figure 3.6a. The TEM image of C-IX-25 (Figure 3.5c) shows the spherical particles of carbon xerogel. At a higher magnification (Figure 3.5c, second row), the wormlike morphology and large amount of micropores are observed, corresponding to the standard isotherm of type Ib obtained from the N_2 adsorption-desorption technique (Figure 3.4 and Table 3.1).

For C-DiX-25, the gelation time was longer while the cluster size was smaller than those of C-DX-25 because polybenzoxazine had a better

interaction with dioxane than with DMF. Systems with better compatibility result in smaller particles and pore size after solvent removal. This explanation is consistent with the proposed model from Pekala [10], Wang et al. [44], and Bock et al. [54] in which mesopores and macropores were created by cluster particles connecting to each other, while solvent was encapsulated to generate pores. Therefore, carbon xerogel with smaller particle size in a dioxane system should have a smaller pore size compared to that of 3D interconnected macroporous carbon xerogel with a bigger particle size in a DMF system. From this result, it was found that C-DX-25 mostly exhibited macropore structure with a small amount of mesopore structure (Table 3.1 and Figure 3.3a). In contrast to C-DX-25, the structure of C-DiX-25 is totally dominated by mesopore structure. However, when comparing the average mesopore diameter, the average mesopore size of C-DX-25 (3.65 nm) was interestingly smaller than that of C-DiX-25 (8.79 nm) even though the average particle size of C-DX-25 was bigger than that of C-DiX-25. These phenomena could be explained by adapting the model proposed by Pekala [10] as mentioned earlier for RF aerogel and that proposed by Wang et al. [56] in which the silica aerogel was built from primary particles with a size of less than one nanometer. The aggregated primary particles, so-called secondary particles, were connected to each other to create porous silica structure.

Our proposed model of carbon xerogel structures created by phase separation process is illustrated in Figure 3.6 along with the SEM micrographs. The primary clusters were smaller clusters initially generated by the phase separation process whereas the secondary clusters were bigger clusters created by the aggregation of primary clusters.

In the case of using DMF as a solvent, the structure of carbon xerogel consisted of both primary and secondary clusters (Figure 3.6a). The primary clusters would aggregate to each other due to poor interaction between the benzoxazine precursor and solvent, resulting in the formation of secondary clusters with a size of 1150 nm as can be seen in the DLS data in Figure 3.2. However, after observation by SEM technique, the particle size of C-DX-25 is around 500-800 nm, which is different than that detected by DLS. There are two proposed reasons for this phenomenon. The first reason is the aggregation of particles. When the particles

aggregate or connect to each other, DLS technique will detect the aggregated size of connected particles. Therefore, the particle size detected by DLS will be slightly larger than that observed by SEM technique. The second reason is the structural shrinkage of PBZ-based organic xerogels after carbonization process. When the 3D interconnected macroporous structure of PBZ-based organic xerogels was carbonized, the particle sizes of PBZ-based organic xerogels as measured by DLS technique would be diminished due to the loss of organic contents, resulting in structural shrinkage. As a result, after carbonization, the particle size of carbon xerogels detected by SEM technique will be slightly smaller than that of organic xerogels observed by DLS technique. The size of clusters or particles could also be detected by another technique such as SAXS, if the cross-position in the scattering curve becomes close to smaller scattering vectors, meaning that the materials have larger particles [54].

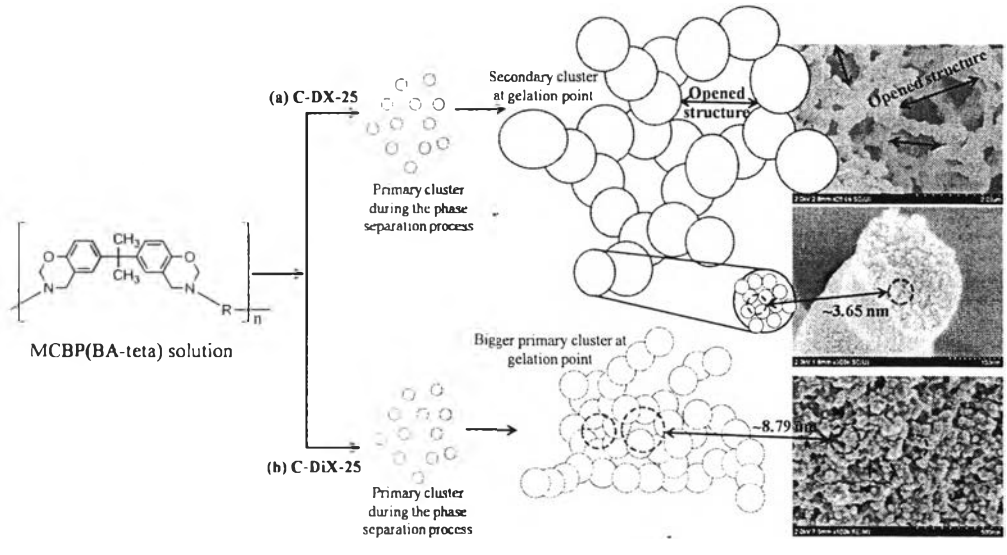

Figure 3.6 Cluster formation during phase separation process (a) C-DX-25 (b) C-DiX-25.

In the DMF system, the aggregated primary clusters generated smaller pores in the range of small mesopores, as reflected by an average mesopore size of 3.65 nm after solvent removal process and carbonization. The secondary clusters further combined to form the final 3D interconnected

macroporous structure containing large amount of macropore volume. The void structure was the consequence of the solvent removal and evaporation of the molecular fragments as a result of carbonization, as illustrated in Figure 3.6a.

In case of C-DiX-25, due to the strong interaction between the benzoxazine precursor and dioxane, the primary clusters with a size of 9.53 nm, detected by DLS, were created during the phase separation process and then continuously grown to be bigger primary clusters. Finally, bigger clusters with an approximate size of 140 nm were obtained and connected with neighboring clusters to form wet organogels encompassing solvent (Figure 3.6b). After the solvent removal process and carbonization, an average mesopore size of 8.79 nm was obtained. In Figure 3.4b, the pore size distributions of C-DiX-25 and C-IX-25 show mesopores and micropores contained inside the structure, respectively. However, the macromore size distribution of C-DX-25 was not provided due to the limitation of Kelvin equation of N_2 adsorption/desorption technique [20, 53].

From all results, we found that the 3D interconnected macroporous carbon xerogel with an extremely large macropore volume, or about 4.33 cm^3/g can be easily produced by using DMF as the solvent during the sol-gel process, without the need of using a hard templating method, acid catalyst, or external ultrasonic irradiation. Moreover, a very short gelation time at ambient conditions (1.15 h) was also observed and an economical ambient pressure drying method could be used for the DMF system without pore collapse due to a poor interaction between benzoxazine and DMF.

In this research, a new method to produce 3D interconnected macroporous carbon xerogel is proposed by using the knowledge of phase separation behavior between benzoxazine and solvent for selecting the solvent species used in the sol-gel process. This new technique, using DMF as a solvent, showed many advantages such as not needing a hard template, a short gelation time within 1.15 h due to the fast formation of extended molecular structure resulting from easier ring-opening polymerization accelerated by DMF itself, and near-zero shrinkage (5-7%) after ambient pressure drying because of the enlarged pore connection in the structure of C-DX-25 as described by Li et al. [57]. However, it should be noted that the structural concept of carbon xerogel is different than that of activated carbon.

Carbon xerogels are the 3D interconnected structure of carbon particles obtained by pyrolysis of 3D interconnected structure of organic particles formed during the sol-gel process [10-12, 20, 44, 54]. Carbon xerogels also exhibit opened end-pores which are useful for mass transfer in certain applications, such as the synthesis of large molecules or the use as a supporting material in continuous flow-through conditions. On the other hand, activated carbon is a microporous material with small pores (<2 nm) located on the surface of carbon [42, 44, 54, 55]. Those small pores in activated carbon are closed end-pores, generated by the loss of structural organic content during the pyrolysis process [42, 44, 54, 55]. The small pores in activated carbon are suitable for certain applications that require both small pores and high surface area. In other words, the applications of carbon xerogels and activated carbons are different and dependent on the required carbon structure for the desired application. Moreover, the micropore volume and surface area of carbon could be easily increased by many activation methods, such as CO_2 activation [42, 58], acidic/basic activation [44, 59, 60], and steam activation [58].

It can be concluded that the use of different solvents for PBZ-based carbon xerogel preparation has significant effects on the properties of the primary particles and how those primary particles interact to form aggregates, as a consequence of its hierarchical structures, leading to various void sizes and distributions.

3.4.2 Effects of resin concentrations

According to Section 3.1, it was found that 3D interconnected macroporous carbon xerogels can be easily produced by using DMF as a solvent with a short gelation time. In this section, the effects of resin concentrations on the 3D interconnected macroporous structure will be studied using DMF as a solvent.

Figure 3.7 shows density and gelation time as a function of benzoxazine concentration. The gelation time increased with increasing benzoxazine concentration. This seemingly contradictory phenomenon can be explained by the solubilizing effect of polybenzoxazine molecules on each other at a higher

concentration. The delayed phase separation caused more fused particles to be able to form after the gelation point.

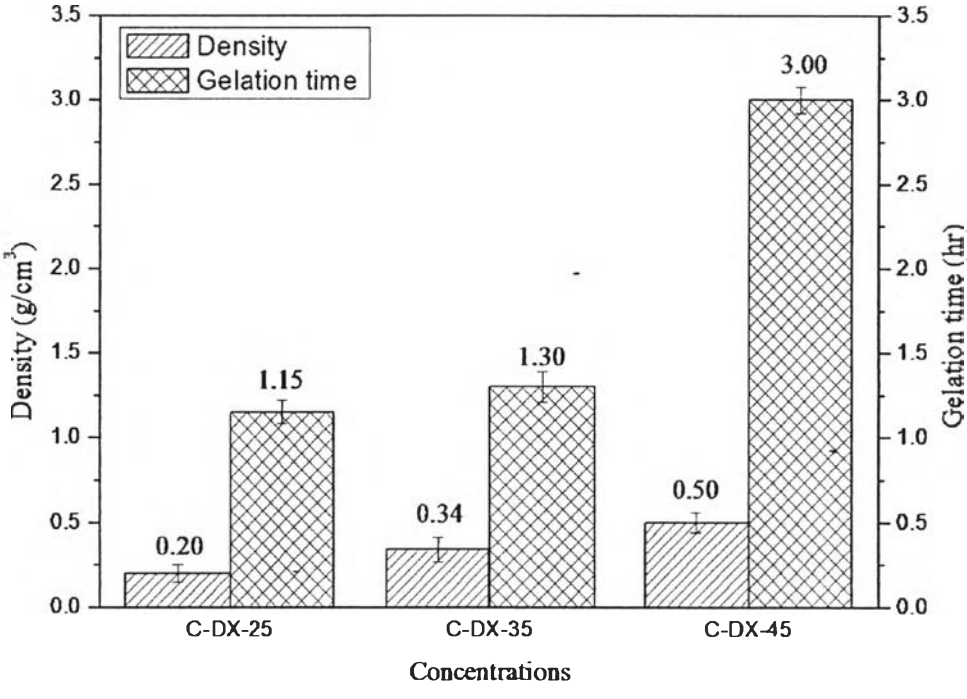

Figure 3.7 Densities and gelation times of carbon xerogels at different concentrations using DMF as a solvent by ambient pressure drying.

FE-SEM micrographs of the samples with different densities are shown in Figure 3.8. It was found that morphologies of all samples indicate densification of the gels at increasing benzoxazine concentrations. Carbon xerogel at concentration of 25% w/w (abbreviated as C-DX-25) and 35% w/w (abbreviated as C-DX-35) clearly shows the 3D interconnected macroporous structures. On the contrary, carbon xerogel at a concentration of 45% w/w (abbreviated as C-DX-45), the particles showed a tendency to fuse together.

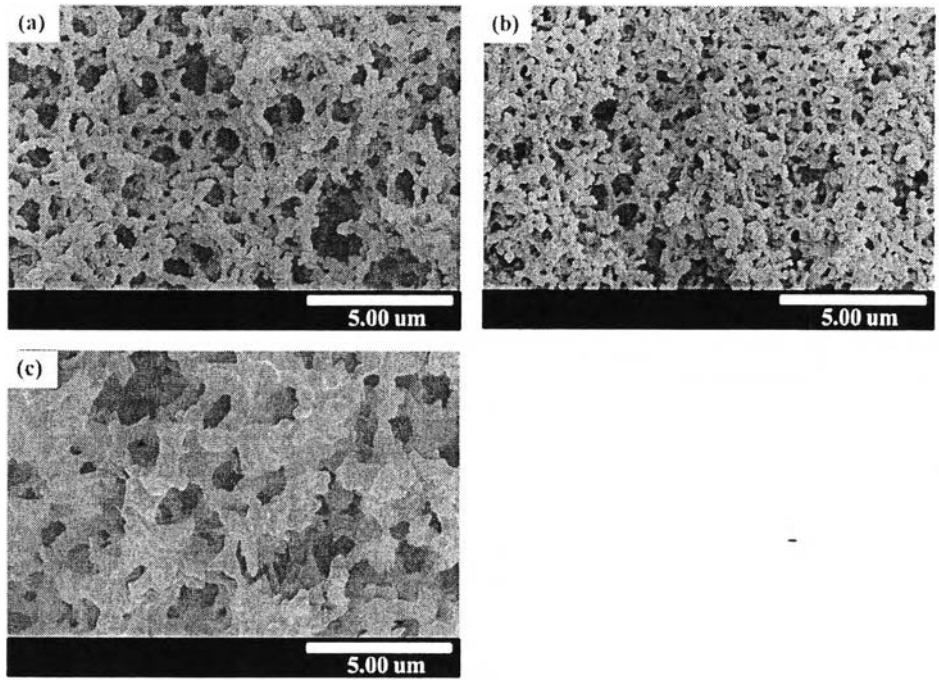

Figure 3.8 SEM micrographs of carbon xerogels using DMF as a solvent by ambient pressure drying (a) C-DX-25 (b) C-DX-35 (c) C-DX-45.

The size of clusters is very important to determine the overall pore morphology of carbon xerogels and its related properties. The N_2 adsorption-desorption isotherms of carbon xerogels prepared from different solid contents are shown in Figure 3.9. According to the IUPAC classification, all samples are found to exhibit the combination of type IIb with a H3 hysteresis loop and type Ic where type Ic represents a microporous adsorbent containing mesopores and type IIb represents a macroporous adsorbent [52, 53, 55]. In addition, no samples reach the plateau region at $p/p_0 \approx 1$ where p_o is the saturation vapor pressure and p the partial pressure at a certain gas volume, implying that large amounts of macropores were contained in the structure of PBZ-based 3D interconnected macroporous carbon xerogels (Figure 3.9a). According to the Kelvin equation [52, 53]:

$$\ln\frac{p}{p_0} = -\frac{2\gamma V_L}{RT}\frac{1}{r_m} \qquad (4)$$

where V_L is the molar volume of liquid adsorptive, γ is the interfacial surface tension at liquid-air interface, r_m is the mean radius of curvature or pore radius, R is the universal gas constant and T is the absolute temperature.

From this equation, we found that the required relative pressures to form N_2-adsorption layers varied directly with the size of pores. The amount of uptake can also be related to pore volume. All samples, especially at a concentration of 35% w/w, show a large amount of adsorption volume at a high relative pressure as shown in Figure 3.9, confirming the presence of small macropores in the structure of 3D interconnected macroporous carbon xerogels. Moreover, all samples also showed similar average mesopore sizes (around 3.57-3.66 nm) as shown in Table 3.2.

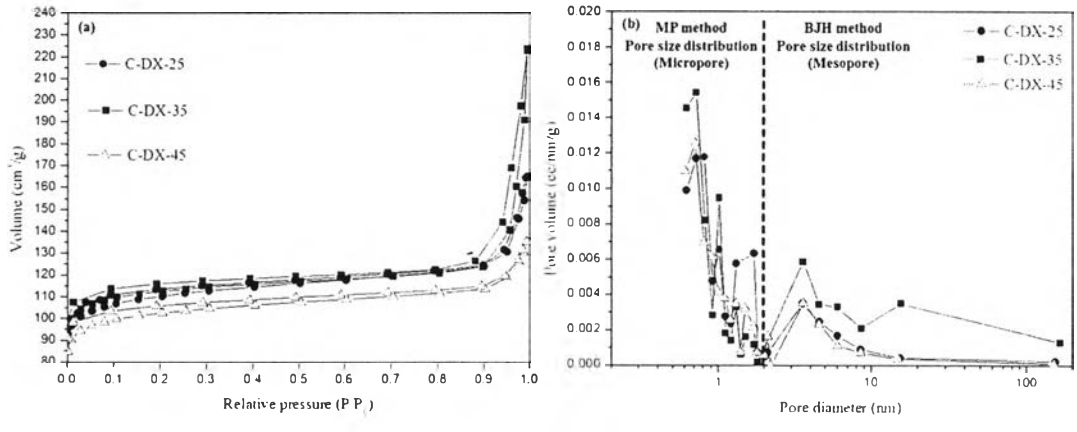

Figure 3.9 (a) N_2 adsorption-desorption isotherms of carbon xerogels using DMF as a solvent at different concentrations (b) pore size distribution.

The details of BET surface area, pore structures, and related properties prepared by different concentrations of polybenzoxazine are tabulated in Table 3.2. The specific micropore volumes of all samples are around 0.14-0.15 cm^3/g. C-DX-35 showed the largest BET surface area, around 341 m^2/g. The macropore volume of all samples is extremely high (4.33 cm^3/g for C-DX-25, 2.17 cm^3/g for C-DX-35, and 1.39 cm^3/g for C-DX-45) and decreases with increasing benzoxazine concentration.

Table 3.2 Pore characteristics of carbon xerogels using DMF as a solvent by ambient pressure drying at different concentrations

Sample	S_{BET} (m^2/g)	S_{micro} (m^2/g)	V_{micro} (cm^3/g)	V_{meso} (cm^3/g)	V_{macro} (cm^3/g)	V_{total} (cm^3/g)	APD_{micro} (nm)	APD_{meso} (nm)
C-DX-25	337	291	0.15	0.08	4.33	4.56	1.16	3.65
C-DX-35	341	271	0.14	0.17	2.17	2.48	1.20	3.66
C-DX-45	312	279	0.14	0.05	1.39	1.58	1.10	3.57

Note : S_{BET} : BET surface area ; S_{micro} : micropore surface area ; V_{micro} : micropore volume ; V_{meso} : mesopore volume ; V_{macro} : macropore volume ; V_{total} : total pore volume ; APD_{micro} : average micropore diameter ; APD_{meso} : average mesopore diameter -

Based on the mixed pore sizes contained in carbon xerogels, the micropore size distribution was calculated by the MP method (Standard Micropore Size Distribution) and the mesopore size distribution by the BJH algorithm [39, 40]. However, the macropore size distribution of all samples was not provided due to the limitation of the Kelvin equation of N_2 adsorption/desorption technique [20, 53]. Figure 3.9b shows the pore size distribution of 3D interconnected macroporous carbon xerogels synthesized from different benzoxazine concentrations. From the graph, we found that micro/mesopore sizes of 3D interconnected macroporous carbon xerogels were in the range of 0.70-150 nm, whereas the peaks of the pore size distribution of all concentrations were in the range of micropores (0.70-1.20 nm) and the peaks of the mesopore size distribution were around 3.66 nm.

The mesopores and macropores could be formed by both the closely packed and the loosely packed carbon nanoparticles [44, 54]. The size of clusters during the gelation process was used to describe the generation of mesopore and macropore volume. Figure 3.10 clearly shows the cluster size at each concentration of benzoxazine during the gelation process. Moreover, the starting size of the clusters at the beginning of the gelation process was different, suggesting that the cluster growth rate and gelation time should be different depending on the concentration of benzoxazine. From the slope of graph in Figure 3.10, we found that the cluster growth rate decreases with increasing concentration. The reasons for these phenomena had already been discussed earlier in the second paragraph of section 3.2.

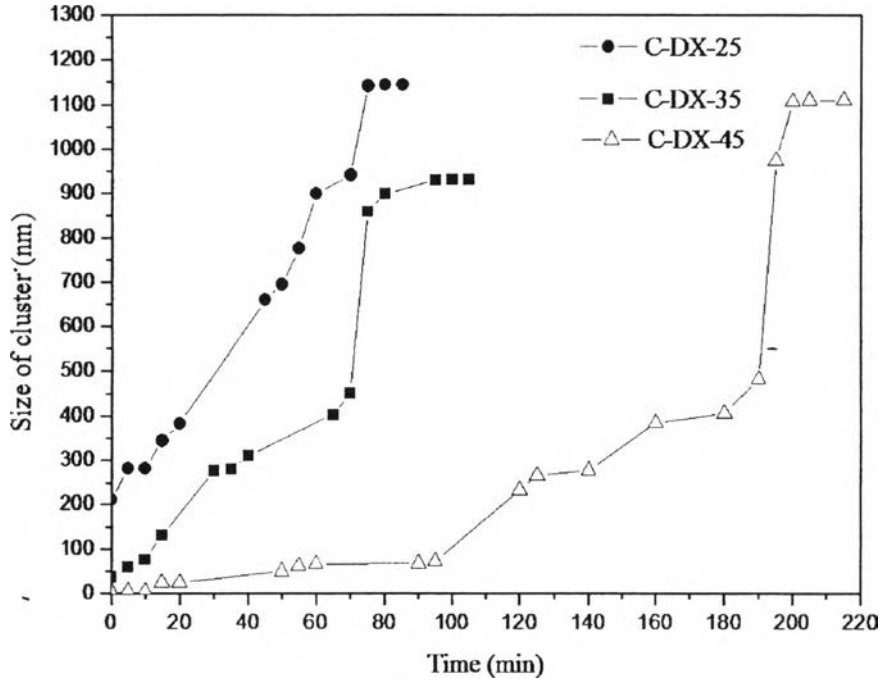

Figure 3.10 Size of cluster during gelation process at different concentrations using DMF as a solvent.

At the pseudo-gelation point measured by the dynamic light scattering technique, C-DX-25 and C-DX-35 show a cluster size around 1150 nm and 930 nm, respectively, leading to a continuously 3D-interconnected macroporous network. Moreover, a large-size aggregation of clustesr in the C-DX-45 sample was observed at the pseudo-gelation point, leading to channel generation (a very open structure) [44, 45, 52, 54].

Upon observation by SEM, the average particle size of C-DX-25 and C-DX-35 was found to be around 500-800 nm, which is different than that detected by DLS. The reasons for this phenomenon are the same as those described in section 3.1.

It can be concluded from the above investigation that an increased concentration of carbon xerogel derived from polybenzoxazine greatly affects the macropore volume of the resulting carbon xerogel and its derivative properties. Moreover, the 3D interconnected macroporous structure of carbon xerogels with extremely large amount of macropore volumes (4.33-2.17 cm^3/g) could be preserved

by varying the benzoxazine concentrations in the range of 25-35%w/w. However, when increasing the concentration to 45% w/w, the particles seem to aggregate to form fused particles and these carbon xerogels show the lowest macropore volume of 1.39 cm^3/g.

3.4.3 Effects of drying methods

For organic and carbon aerogel preparations, the supercritical CO_2 drying method was used to remove the solvents in order to prevent pore collapse of mesopores and macropores [10-12]. Although the pore structure of gels could be maintained by supercritical CO_2 drying, this method has many disadvantages such as high cost, low production rate due to multiple steps required, high energy consumption, and large time consumption.

The purpose of this section is to look for a solvent that has a poor interaction with benzoxazine so an economical ambient pressure drying method can be used as effectively as the supercritical CO_2 drying method. In other words, we want to discover which solvent can provide the same pore structure of organic/carbon gel after solvent removal process by both ambient pressure drying and super critical CO_2 drying methods. According to section 3.1, the structure of organic xerogel was collapsed by the ambient pressure drying method when dioxane was used as a solvent. Theoretically, although the structure of organic xerogel in a dioxane system can be preserved by super critical CO_2 drying, dioxane is not appropriate for ambient pressure drying as observed in section 3.1 and is out of the scope of our research. Therefore, the effects of super critical CO_2 drying method will not be studied for a dioxane system and the θ-solvent for benzoxazine like DMF will be hereinafter used for studying the effects of drying methods. The condition with the highest amount of mesopore and macropore volumes, at a benzoxazine concentration of 35% w/w using DMF as a solvent, was selected for these drying studies.

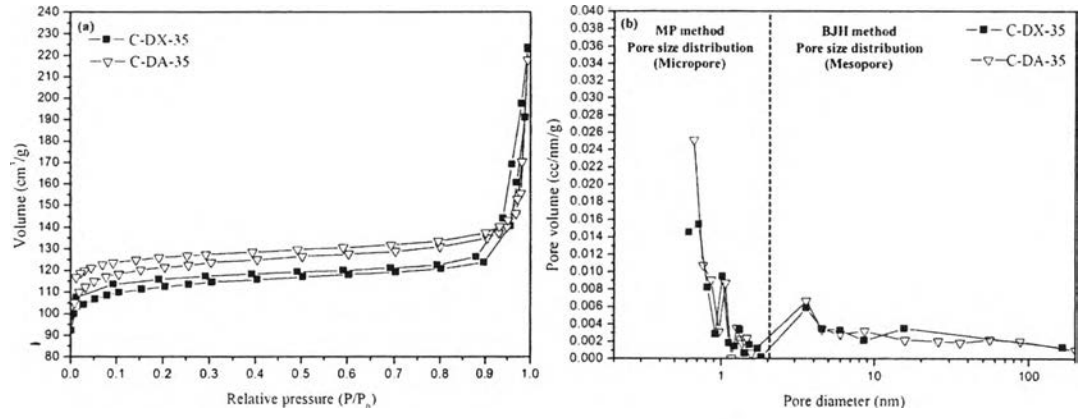

Figure 3.11 (a) N_2 adsorption-desorption isotherms of carbon xerogels using DMF as a solvent by (a) ambient pressure drying (C-DX-35) and supercritical CO_2 drying (C-DA-35) (b) pore size distribution.

The resulting carbon obtained from supercritical CO_2 drying is abbreviated as C-DA-35 in which A stands for aerogel. Figure 3.11a shows the adsorption isotherms of C-DA-35, representing the combination of the adsorption isotherms type IIb with a H3 hysteresis loop and type Ic [52, 53, 55]. The adsorption isotherms of both C-DA-35 and C-DX-35 did not reach the plateau region at a high relative pressure ($p/p_0 \approx 1$), indicating a macropore regime in the sample. In addition, the adsorption isotherms of C-DA-35 in Figure 3.11a show a higher adsorption volume at a relative pressure of less than 0.1 (micropore regime) than that of C-DX-35. This higher adsorption volume of C-DA-35 in the micropore regime indicates C-DA-35 has a slightly higher micropore volume than C-DX-35. However, in the mesopore regime, the adsorption volume curves of both samples are slightly different and show a similar slope. Therefore, the distinction between the two isotherms in Figure 3.11a is mainly affected by the adsorption of micropores at low relative pressures.

The pore characteristics of C-DA-35 are surprisingly similar to those of C-DX-35, as summarized in Table 3.3. However, the specific surface area of C-DA-35 calculated from the BET algorithm is slightly higher than that of C-DX-35 (around 370 and 341 m^2/g respectively). In addition, the micropore surface area of C-DA-35 is significantly higher at 326 m^2/g than C-DX-35 at 271 m^2/g due to the

increased micropore volume of C-DA-35. The mesopore volume and mesopore size of C-DX-25 and C-DA-25 are almost the same, at about 0.17 and 0.15 cm^3/g, 3.66 and 3.57 nm, respectively. Moreover, both samples possess extremely large macropore volumes, at about 2.15-2.17 cm^3/g. The micro- and mesopore size distributions of both samples are in similar ranges (Figure 3.11b). Furthermore, the same 3D interconnected macroporous structure was clearly observed in C-DX-35 and C-DA-35 by SEM (Figure 3.12). Therefore, different drying methods have no significant effect on the morphology of PBZ-derived carbon gel. This result could be explained by the structure of polybenzoxazine and the surface tension at the interface between polymer and solvent.

Table 3.3 Pore characteristics of carbon xerogels using DMF as a solvent at 35% w/w of solid contents by ambient pressure drying and supercritical CO_2 drying

Sample	S_{BET} (m^2/g)	S_{micro} (m^2/g)	V_{micro} (cm^3/g)	V_{meso} (cm^3/g)	V_{macro} (cm^3/g)	V_{total} (cm^3/g)	APD_{micro} (nm)	APD_{meso} (nm)
C-DX-35	341	271	0.14	0.17	2.17	2.48	1.20	3.66
C-DA-35	370	326	0.17	0.15	2.15	2.47	1.28	3.57

Note : S_{BET} : BET surface area ; S_{micro} : micropore surface area ; V_{micro} : micropore volume ; V_{meso} : mesopore volume ; V_{macro} : macropore volume ; V_{total} : total pore volume ; APD_{micro} : average micropore diameter ; APD_{meso} : average mesopore diameter

To explain the preservation of pore structure in the samples, the Laplace equation was used as described by Wu et al. [61]. According to the Laplace equation [52, 53, 62]:

$$\Delta p = \frac{2\gamma \cos\theta}{r} \tag{5}$$

where Δp is the capillary pressure, γ is the interfacial surface tension at liquid-air interface, θ is the contact angle and r is the radius of the capillary. Normally, supercritical CO_2 drying is used to remove the solvent without pore collapse because this method creates no surface tension (γ) and capillary pressure (Δp). Judging from the poor interaction between benzoxazine and DMF, and the Laplace equation (Eq.5)

[52, 53, 61], the surface tension between benzoxazine and DMF in an ambient pressure drying process should be minimized, resulting in a low capillary force. By minimizing capillary force, the structural collapse of C-DX-35 could be minimized. The similar pore characteristics of C-DX-35 and C-DA-35 can also be explained by the structure of polybenzoxazine itself.

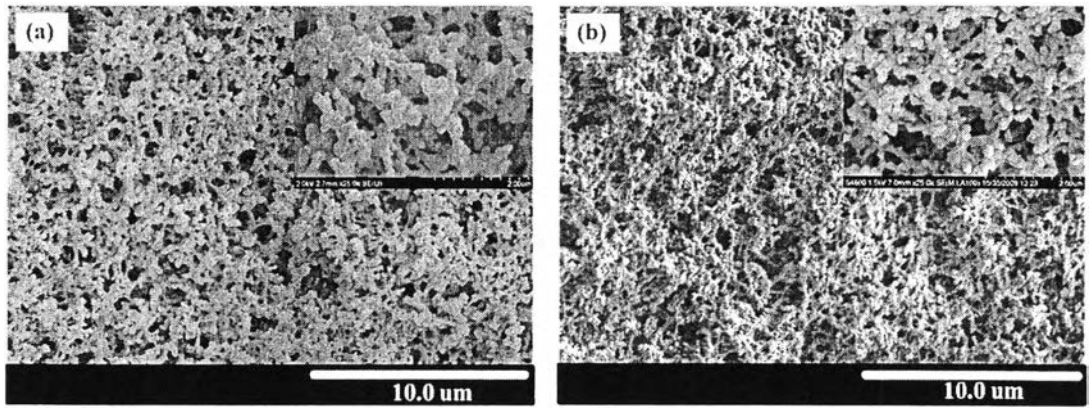

Figure 3.12 SEM micrographs of porous carbon using DMF as a solvent by (a) ambient pressure drying (C-DX-35) and (b) supercritical CO_2 drying (C-DA-35); inset: high magnification.

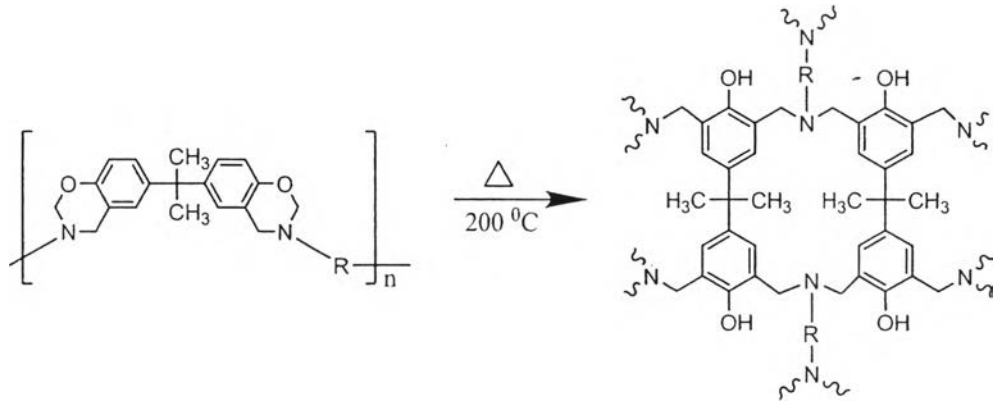

Figure 3.13 Structure of MCBP(BA-teta) and cross linked MCBP(BA-teta).

Figure 3.13 illustrates the structure of MCBP(BA-teta) and crosslinked MCBP(BA-teta). Cross-linked MCBP(BA-teta) has high strength and modulus [21-25] due to the chemical cross-links by covalent bonds and physical cross-links by various forms of hydrogen bonds. Such a cross-link structure would withstand pore collapse generated by the capillary force at the interface between the pore wall and liquid solvent, leading to near-zero linear shrinkage after ambient pressure drying. On the other hand, dioxane was not appropriate for ambient pressure drying due to strong interaction between the benzoxazine precursor and dioxane. The linear shrinkage of C-DiX-25 was about 30% during ambient pressure drying. By using isopropanol and DMF as solvents, spherical particles (C-IX-25) and 3D interconnected macroporous carbon xerogel (C-DX-25) show near-zero shrinkage at approximately 5% and 5-7%, respectively, after ambient pressure drying. This near-zero shrinkage was due to the enlarged pore connection in the structure of both samples as described by Li et al. [57]. In short, for the ambient drying to be successful, the choice of solvent is recommended to be close to the θ-solvent. Such mediocre solvent that dissolves benzoxazine resin but not good enough to resist phase separation would lead to nearly identical xerogel morphology as that obtained by the supercritical CO_2 method despite the use of much easier ambient drying.

3.5 Conclusions

MCBP(BA-teta)-based carbon xerogels with different properties were obtained by varying different synthesis parameters. The gelation time and density increased with increasing precursor concentrations. Furthermore, the benzoxazine precursor also showed a fast gelation time in the DMF system about 1.15-3.00 h due to fast ring-opening polymerization accelerated by the hydrophilic solvent. The rate of cluster growth at lower precursor concentrations of PBZ was faster than those of higher precursor concentrations for the DMF system. The specific surface area, mesopore volume, and macropore volume could be tailored by varying the concentrations of benzoxazine. Interestingly, 3D interconnected macroporous carbon xerogels with extremely large amount of macropore volumes (1.39-4.33 cm^3/g) could be easily obtained after carbonization by using DMF as the solvent via self-formation

of benzoxazine during the sol-gel process. Moreover, carbon xerogels could obviously keep their 3D interconnected macroporous structure at a concentration of 25-35% w/w.

Interestingly, by using different types of solvents, different morphology and porous characteristics were achieved. The spherical particles with a microporous property obtained from a self-micelle-like formation model were observed by using isopropanol as the solvent. By using dioxane as the solvent, C-DiX-25 showed the characteristics of mesoporous carbon due to the interconnection of small clusters of benzoxazine. Therefore, the properties of MCBP(BA-teta)-based carbon xerogels can be easily changed to micro-, meso-, or macroporous properties by changing the solvent species during the sol-gel process.

In comparing the rate of cluster growth between the DMF and dioxane systems, the rate of cluster growth in the dioxane system was slower than that of the DMF system, implying good miscibility between PBZ and dioxane. During the phase separation process, primary clusters were formed and continuously grew in size until the gelation point was achieved if dioxane was used. However, the primary clusters could agglomerate to form the secondary clusters, resulting in a 3D interconnected macroporous structure for the DMF system. Without the need of a supercritical CO_2 drying method, in the DMF system, MCBP(BA-teta) based-xerogel was sufficiently strong to withstand pore collapse during the ambient pressure drying method.

All results suggest that DMF and polybenzoxazine are an appropriate solvent and excellent candidate resin, respectively, for producing 3D interconnected macroporous carbon xerogel with extremely large amount of macropore volumes (1.39-4.33 cm^3/g). Additionally, this system does not require a template, external ultrasonic vibrations, or an acid catalyst which could lead to extensive energy and time consumptions, resulting in high production costs. More generally, it was found that choice of the θ-solvent for the polymer allows the adoption of ambient pressure drying without concerns for pore collapse caused by capillary force.

3.6 Acknowledgements

This work has been financially supported by the Petroleum and Petrochemical College and the Center of Excellence on Petrochemical and Materials Technology, Chulalongkorn University. The authors would like to thank Prof. Suwabun Chirachanchai for his kind support on the DLS apparatus. In addition, special thanks also go to the Office of Higher Education Commission for her support of the National Research University Program (WCU-048-CC-57).

3.7 References

[1] Chen SX, Zhang X, Shen PK (2006) Macroporous conducting matrix: Fabrication and application as electrocatalyst support, Electrochem Commun 8:713-719.

[2] Liang C, Dai S, Guiochon G (2003) A graphitized-carbon monolithic column, Anal Chem 75:4904-4912.

[3] Tonanon N, Siyasukh A, Wareenin Y, Charinpanitkul T, Tanthapanichakoon W, Nishihara H et al (2005) 3D interconnected macroporous carbon monoliths prepared by ultrasonic irradiation, Carbon 43:2808-2811.

[4] Tonanon N, Wareenin Y, Siyasukh A, Tanthapanichakoon W, Nishihara H, Mukai SR et al (2006) Preparation of resorcinol formaldehyde (RF) carbon gels: Use of ultrasonic irradiation followed by microwave drying, J Non-Cyst Solids 352:5683-5686.

[5] Siyasukh A, Maneeprom P, Larpkiattaworn S, Tonanon N, Tanthapanichakoon W, Tamon H et al (2008) Preparation of a carbon monolith with hierarchical porous structure by ultrasonic irradiation followed by carbonization, physical and chemical activation, Carbon 46:1309-1315.

[6] Bu H, Rong J, Yang Z (2002) Template synthesis of polyacrylonitrile-based ordered macroporous materials and their derivetives, Macromol Rapid Commun 23:460-464.

[7] Baumann TF and Satcher Jr JH (2004) Template-directed synthesis of periodic macroporous organic and carbon aerogels, J Non-Cryst Solids 350:120-125.

[8] Taguchi A, Smatt JH, Linden M (2003) Carbon monoliths possessing a hierarchical, fully interconnected porosity, Adv Mater 15:1209-1211.

[9] Wang X, Bozhilov KN, Feng P (2006) Facile preparation of hierarchically porous carbon monoliths with well-ordered mesostructures, Chem Mater 18:6373- 6381.

[10] Pekala RW (1989) Organic aerogels from the polycondensation of resorcinol with formaldehyde, J Mater Sci 24:3221-3227.

[11] Tamon H, Ishizaka H, Mikami M, Okazaki M (1997) Porous structure of organic and carbon aerogels synthesized by sol-gel polycondensation of resorcinol with formaldehyde, Carbon 35:791-796.

[12] Pekala RW and Schaefer DW (1993) Structure of organic aerogels. 1. Morphology and scaling, Macromolecules 26:5487-5493.

[13] Qin G and Guo S (2001) Preparation of RF organic aerogels and carbon aerogels by alcoholic sol-gel process, Carbon 39:1935-1937.

[14] Liang C, Sha G, Guo S (2000) Resorcinol-formaldehyde aerogels prepared by supercritical acetone drying, J Non-Cryst Solids 271:167-170.

[15] Qin G, Wei W, Guo S (2003) Semi-continuous drying of RF gels with supercritical acetone, Carbon 41:851-853.

[16] Tamon H, Ishizaka H, Yamamoto T, Suzuki T (1999) Preparation of mesoporous carbon by freeze drying, Carbon 37:2049-2055.

[17] Arbizzani C, Beninati S, Manferrari E, Soavi F, Mastragostino M (2007) Cryo- and xerogel carbon supported PtRu for DMFC anodes, J Power Sources 172:578-586.

[18] Liu N, Zhang S, Fu R, Dresselhaus MS, Dresselhaus G (2006) Carbon aerogel spheres prepared via alcohol supercritical drying, Carbon 44:2430-2436.

[19] Shen J, Hou J, Guo Y, Xue H, Wu G, Zhou B (2005) Microstructure control of RF and carbon aerogels prepared by sol-gel process, J Sol-Gel Sci Technol 36:131-136.

[20] Job N, Thery A, Pirard R, Marien J, Kocon L, Rouzaud JN et al (2005) Carbon aerogels, cryogels and xerogels: Influence of the drying method on the textural properties of porous carbon materials, Carbon 43:2481-2494.

[21] Ning X and Ishida H (1994) Phenolic materials via ring-opening polymerization: Synthesis and characterization of bisphenol-A based benzoxazines and their polymers, J Polym Sci, Part A: Polym Chem 32:1121-1129.

[22] Ghosh NN, Kiskan B, Yagci Y (2007) Polybenzoxazines-New high performance thermosetting resins: Synthesis and properties, Prog Polym Sci 32:1344-1391.

[23] Ishida H and Allen DJ (1996) Mechanical characterization of copolymers based on benzoxazine and epoxy, Polymer 37:4487-4495.

[24] Agag T and Takeichi T (2007) High-molecular-weight AB-type benzoxazines as new precursors for high-performance thermosets, J Polym Sci, Part A: Polym Chem 45:1878-1888.

[25] Ishida H (2011) Overview and historical background of polybenzoxazine research, in: H. Ishida, T. Agag (Eds.), Handbook of Benzoxazine Resins, Elsevier, Amsterdam, pp. 3-81.

[26] Lorjai P, Chaisuwan T, Wongkasemjit S (2009) Porous structure of polybenzoxazine-based organic aerogel prepared by sol-gel process and their carbon aerogels, J Sol-Gel Sci Technol 52:56-64.

[27] Katanyoota P, Chaisuwan T, Wongchaisuwat A, Wongkasemjit S (2010) Novel polybenzoxazine-based carbon aerogel electrode for supercapacitors, Mater Sci Eng, B 167:36-42.

[28] Rubenstein DA, Lu HB, Mahadik SS (2012) Characterization of the physical properties and biocompatibility of polybenzoxazine-based aerogels for use as a novel hard-tissue scaffold, J Biomater Sci, Polym Ed 23:1171-1184.

[29] Thubsuang U, Ishida H, Wongkasemjit S, Chaisuwan T (2012) Novel template confinement derived from polybenzoxazine-based carbon xerogels for synthesis of ZSM-5 nanoparticles via microwave irradiation, Micropor Mesopor Mater 156:7-15.

[30] Zipfel J, Berghausen J, Schmidt G, Lindner P, Alexandridis P, Tsianou M et al (1999) Shear induced structures in lamellar phases of amphiphilic block copolymers, Phys Chem Chem Phys 1:3905-3910.

[31] Alexandridis P and Yang L (2000) SANS investigation of polyether block copolymer micelle structure in mixed solvents of water and formamide, ethanol, or glycerol, Macromolecules 33:5574-5587.

[32] Antoniou E and Alexandridis P (2010) Polymer conformation in mixed aqueous-polar organic solvents, Eur Polym J 46:324-335.

[33] Holmqvist P, Alexandridis P, Lindman B (1997) Phase behavior and structure of ternary amphiphilic block copolymer-alkanol-water systems: Comparison of poly(ethylene oxide)/poly(propylene oxide) to poly(ethylene oxide)/poly(tetrahydrofuran) copolymers, Langmuir 13:2471-2479.

[34] Ishida H (1996) Process for preparation of benzoxazine compounds in solventless systems. US Pat 5543516.

[35] Takeichi T, Kano T, Agag T (2005) Synthesis and thermal cure of high molecular weight polybenzoxazine precursors and the properties of the thermosets, Polymer 46:12172-12180.

[36] Thubsuang U, Ishida H, Wongkasemjit S, Chaisuwan T (2014) Improvement in the pore structure of polybenzoxazine-based carbon xerogels through a silica templating method, J Porous Mater. doi: 10.1007/s10934-014-9786-7

[37] Brunauer S, Emmett PH, Teller E (1938) Adsorption of gases in multimolecular layers, J Am Chem Soc 60:309-319.

[38] Lippens BC and Boer JH de (1965) Studies on pore systems in catalysts: V. The *t* method, J Catal 4:319-323.

[39] Barrett EP, Joyner LG, Halenda PP (1951) The determination of pore volume and area distributions in porous substances. I. Computations from nitrogen isotherms, J Am Chem Soc 73:373-380.

[40] Joyner LG, Barrett EP, Skold R (1951) The determination of pore volume and area distributions in porous substances. II. Comparison between nitrogen isotherm and mercury porosimeter methods, J Am Chem Soc 73:3155-3158.

[41] Horikawa T, Hayashi J, Muroyama K (2004) Controllability of pore characteristics of resorcinol-formaldehyde carbon aerogel, Carbon 42:1625-1633.

[42] Rodriguez-Reinoso F, Lopez-Gonzalez JD, Berenguer C (1982) Activated carbons from almond shells-I. Preparation and characterization by nitrogen adsorption, Carbon 20:513-518.

[43] Wu D, Fu R, Dresselhaus MS, Dresselhaus G (2006) Fabrication and nano structure control of carbon aerogels via a microemulsion-templated sol-gel polymerization method, Carbon 44:675-681.

[44] Wang J, Yang X, Wu D, Fu R, Dresselhaus MS, Dresselhaus G (2008) The porous structures of activated carbon aerogels and their effects on electrochemical performance, J Power Sources 185:589-594.

[45] Long D, Liu X, Qiao W, Zhang R, Zhan L, Ling L (2009) Molecular design of polymer precursors for controlling microstructure of organic and carbon aerogels, J Non-Cryst Solids 355:1252-1258.

[46] Hildebrand JH and Scott RL (1949) The Solubility of Non-Electrolytes 3rd ed. Dover, New York

[47] Koenhen DM and Smolders CA (1975) The determination of solubility parameters of solvents and polymers by means of correlations with other physical quantities, J Appl Polym Sci 19:1163-1179.

[48] Wang X, Wang X, Liu L, Bai L, An H, Zheng L et al (2011) Preparation and characterization of carbon aerogel microspheres by an inverse emulsion polymerization. J Non-Cryst Solids 357:793-797.

[49] Yamamoto T, Sugimoto T, Suzuki T, Mukai SR, Tamon H (2002) Preparation and characterization of carbon cryogel microshpheres, Carbon 40:1345-1351.

[50] Kim SI, Yamamoto T, Endo A, Ohmori T, Nakaiwa M (2006) Influence of nonionic surfactant concentration on physical characteristics of resorcinol-formaldehyde carbon cryogel microspheres, J Ind Eng Chem 12:484-488.

[51] Wang X, Liu L, Wang X, Bai L, Wu H, Zhang X et al (2011) Preparation and performances of carbon aerogel microspheres for the application of supercapacitor, J Solid State Electrochem 15:643-648.

[52] Gregg SJ and Sing KSW (1982) Adsorption, Surface Area and Porosity 2nd ed. Academic Press, London

[53] Rouquerol F, Rouquerol J, Sing KSW (1999) Adsorption by Powders and Porous Solids, Principles, methodology and Applications. Academic Press, London

[54] Bock V, Emmerling A, Saliger R, Fricke J (1997) Structural investigation of resorcinol formaldehyde and carbon aerogels using SAXS and BET, J Porous Mater 4:287-294.

[55] Guzel F and Uzun I (2002) Determination of the micropore structures of activated carbons by adsorption of various dyestuffs from aqueous solution, Turk J Chem 26:369-377.

[56] Wang J, Shen J, Zhou B, Deng Z, Zhao L, Zhu L et al (1998) Cluster structure of silica aerogel investigated by laser ablation, Nanostruct Mater 10:909-916.

[57] Li WC, Lu AH, Schuth F (2005) Preparation of monolithic carbon aerogels and investigation of their pore interconnectivity by a nanocasting pathway, Chem Mater 17:3620-3626.

[58] Gorka J and Jaroniec M (2011) Hierarchically porous phenolic resin-based carbons obtained by block copolymer-colloidal silica templating and post-synthesis activation with carbon dioxide and water vapor, Carbon 49:154-160.

[59] Conceicao FL, Carrott PJM, Ribeiro Carrott MML (2009) New carbon materials with high porosity in the 1–7 nm range obtained by chemical activation with phosphoric acid of resorcinol–formaldehyde aerogels, Carbon 47:1867-1885.

[60] Park HW, Kim JK, Hong UG, Lee YJ, Choi JH, Bang Y et al (2013) Catalytic decomposition of 1,3-diphenoxybenzene to monomeric cyclic compounds over palladium catalysts supported on acidic activated carbon aerogels, Appl Catal, A 456:59-66.

[61] Wu D, Fu R, Zhang S, Dresselhaus MS, Dresselhaus G (2004) Preparation of low-density carbon aerogels by ambient pressure drying, Carbon 42:2033-2039.

[62] Zarzycki J, Prassas M, Phalippou J (1982) Synthesis of glasses from gels: the problem of monolithic gels, J Mater Sci 71:3371-3379.